ELSEVIER

Journal of Nuclear Materials 241-243 (1997) 1065-1070

journal of nuclear materials

Isotope effects in hydrogen retention of graphite and beryllium irradiated simultaneously with dual H^+ and D^+ beams

B. Tsuchiya *, K. Morita

Department of Crystalline Materials Science, School of Engineering, Nagoya University, Furo-cho, Chikusa-ku, Nagoya 464-01, Japan

---

Abstract

The concentration profiles of H and D retained in graphite at temperatures from room temperature to 900 K and beryllium at room temperature by simultaneous dual H^+ and D^+ ion implantation have been measured by means of an elastic recoil detection (ERD) technique. It has been found that as the fluence increases, the concentrations of H and D retained in graphite and beryllium increase at the same rate in the beginning of the implantation and hereafter that of H saturates faster than that of D. The concentration ratios of D to H retained in graphite and beryllium n_T^D/n_T^H, at steady state were determined to be 1.8 ± 0.2 and 1.25 ± 0.2, respectively. The steady state values of n_T^D/n_T^H for graphite at room and high temperatures and beryllium at room temperature have been also calculated to be 1.5 ± 0.2, 1.5 ± 0.2 and 1.3 ± 0.2, respectively, by solving a set of mass balance equations for H and D under simultaneous H^+ and D^+ ion implantation. The experimental and theoretical values are compared and discussed.

Keywords: Particle balance; Low Z wall material; Wall particle retention

---

1. Introduction

In magnetically confined fusion devices where low Z number materials such as carbon, boron and beryllium are used as plasma facing components, the production of fusion power of 1-10 MW in D-T discharge experiments has been demonstrated [1,2]. The low Z materials have operated under wall pumping for retaining large amounts of hydrogen isotopes. During the long term discharge they would operate under wall fueling due to hydrogen re-emission. In order to achieve the ignition condition during long term D-T discharge, it is of essential importance to evaluate and predict the transient recycling fluxes of each hydrogen species from the plasma facing components and control the D/T ratio in the fueling.

For this purpose, so far, the elementary processes related to the retention and re-emission of hydrogen isotopes in low Z materials have been extensively studied by means of an ion beam analysis by many authors [3-11]. Several models have been proposed for trapping and molecular recombination [6-11]. For evaluation of the transient recycling of hydrogen isotopes from graphite, the mass balance equations have been proposed by several authors [12-15], in which the retention and re-emission are described in terms of elementary processes, for instance, such as diffusion, trapping, thermal and ion-induced detrapping, local molecular recombination and local hydrocarbon formation [13]. In the last two papers [14,15], the diffusion of hydrogen isotopes in crystallites of polycrystalline targets and their surface molecular recombination have been more accurately taken into account, which is so called two-region-model [15]. The mass balance equations not including the diffusion term and the surface molecular recombination, but the local molecular recombination and local hydrocarbon formation described in terms of the diffusion-limited reaction model can be regarded to be an approximation of

---

[*] Corresponding author. Fax: +81-52 789 3791; e-mail: k-morita@mail.nucl.nagoya-u.ac.jp.

PII S0022-3115(96)00661-7

the two-region-model, which are applicable for polycrystalline target of small crystallites. Recently, the present authors have shown that there exists large isotope difference between the concentrations of H and D retained in graphite at room temperature by simultaneous H^+ and D^+ ion implantation, which is reasonably explained in terms of the mass balance equations with the local molecular recombination [14]. Their further applications to the elevated temperatures and other targets are interesting.

In this paper, we report the temperature dependence of the difference between the concentrations of H and D retained in graphite by simultaneous H^+ and D^+ ion implantation. Moreover, we report the difference between the concentrations of H and D retained in beryllium at room temperature. The difference between the n_T^D/n_T^H ratios in graphite and beryllium is discussed using the mass balance equations.

2. Experiments

The specimens used were an isotopic graphite plate (IG110U) of $10 \times 15 \times 1$ mm^3 in size and a beryllium disc (Bruch-Wellman) of 30 mm in diameter and 1 mm in thickness and of 99 at% in purity. The oxygen content measured by RBS (Rutherford backscattering spectroscopy) for beryllium was 0.93% and little heavier impurities were included in the bulk. The specimens were placed in contact with a ceramic heater on a manipulator in a UHV chamber which was usually evacuated to a base pressure less than 4×10^{-7} Pa. The temperature was measured with a thermocouple in contact with the surface. The residual hydrogen atoms in the graphite and beryllium specimens were removed out by heating them at 1270 K for 40 min and at 950 K for 10 min, respectively. The oxidized layers on the beryllium surface were removed by 0.5 keV Ar^+ sputter at the angle of 60° to the surface normal before every implantation of hydrogen isotopes.

The graphite and beryllium specimens were irradiated simultaneously with 4 keV H_2^+ and 3 keV D_2^+ ions at the angles of 20° and 35° to the surface normal, respectively, so that the peak depths of both ions in the target coincided with each other [17]. Both ion beams were separately generated from two differentially pumped ion guns of the same type and the working pressure was around 3×10^{-5} Pa. The fluxes of H^+ and D^+ ions on the target were measured with a movable small Faraday cup placed beneath the target assembly and were independently selected to be 4.3×10^{13} ions/cm^{2}s. Implantation temperature of beryllium was room temperature and that of graphite ranged from 300 K to 900 K.

The concentrations of H and D retained in the specimens were measured after several stages of implantation by means of the ERD (elastic recoil detection) technique with a He^+ ion probe beam of 1.7 MeV. The He^+ fluence was simultaneously monitored by means of the RBS technique.

3. Experimental results

The specimens of graphite and beryllium were simultaneously irradiated with dual ion beams of 3 keV D_2^+ and 4 keV H_2^+ ions up to saturation and the concentrations of H and D retained were measured at several stage of the irradiation by means of the ERD technique. It was found that as the ion fluence increases both concentrations of H and D increase and reach a steady state. The steady state ERD spectra for graphite specimens at different temperatures are shown in Fig. 1. It is

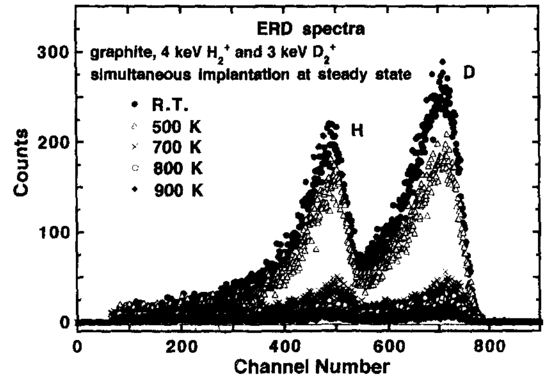

Fig. 1. Steady state ERD spectra of H and D retained in graphite by simultaneous 4 keV H_2^+ and 3 keV D_2^+ irradiation at temperatures from RT to 900 K.

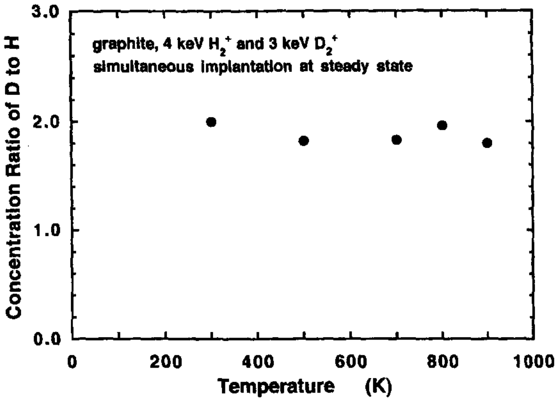

Fig. 2. Temperature dependence of the steady state concentration ratio of D to H retained in graphite, n_T^D / n_T^H.

seen from Fig. 1 that the peak heights of H and D decrease as the temperature increases. The ratios of the relative concentrations estimated from the H and D peak heights averaged over 40 channels are plotted as a function of temperature in Fig. 2. The relative concentrations of H and D to C were calculated from the peak height using He^+ fluence, the solid angle of the detector, the recoil cross-sections of He^+ ion for H and D [18] and the stopping cross-sections for H^+, D^+ and He^+ ions [17] by the standard analysis technique. Since the peak depths of H and D from the target surface are the same, the error in the D/H ratio is estimated to be less than 10%, which is mainly ascribed to uncertainty in the recoil cross-sections. The contribution of a low energy tail of the D peak to the H peak, seen in Fig. 1, was subtracted using the ERD spectrum measured on the independent irradiation of D_2^+ ion beam at the same energy, of which the peak height is the same as the D peak height. It is seen from Fig. 2 that the D/H ratio is almost a constant of 1.8 ± 0.2 against the temperature change.

The relative concentrations of H and D retained in beryllium at room temperature are shown as a function of irradiation time in Fig. 3. It is seen from Fig. 3 that similarly to graphite, the concentrations of H and D increase at the same rate in the beginning of the irradiation and the average D/H ratio on saturation is 1.25.

4. Discussion

In Section 3 it was found that the ratio of D to H retained in graphite by simultaneous H^+ and D^+ implantation is 1.8 independent of the temperature in the range from RT to 900 K, which is a strong isotope difference. The ratio of D to H in beryllium was found to be 1.25 at room temperature. The D/H ratios in graphite and in beryllium are discussed using the mass balance equations.

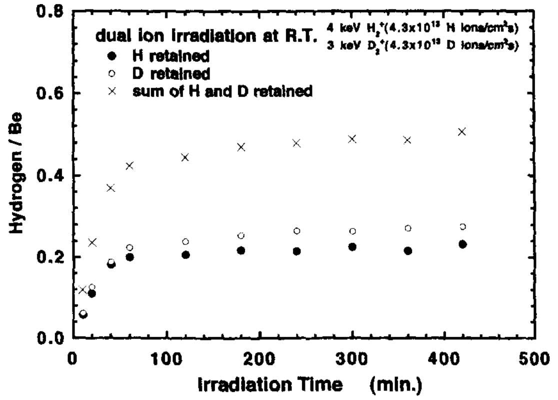

Fig. 3. Transient curves of the concentrations of H and D (hydrogen/Be) retained in beryllium by simultaneous 4 keV H_2^+ and 3 keV D_2^+ irradiation at room temperature.

4.1. The mass balance equations under simultaneous dual H^+ and D^+ ion implantation

In the mass balance equations for generally calculating the transient recycling fluxes of hydrogen isotopes, the elementary processes such as diffusion, source, trapping, detrapping, local molecular recombination and local formation of hydrogen-target atom complex molecule are taken into account [13]. When the diffusion constants of hydrogen isotopes are not so large and the diffusion-limited reaction model is used for the trapping, local molecular recombination and hydrocarbon molecule formation, the diffusion term may be dropped, for simplicity, because the rate constants include the diffusion constant. The targets implanted with energetic ions up to saturation (or a steady state) are heavily damaged and modified into complex textures which are composed of small crystallites of a few tens of nanometer in size for graphite and include small cavities, voids and bubbles for beryllium at room temperature. For graphite in such a state, the mass balance equations with local molecular recombination and local hydrocarbon formation have explained reasonably the isothermal re-emission curves of H and D retained by independent ion implantation [19,20]. The mass balance equations may be applicable for beryllium because the thermal re-emission rate is independent of the depth [21]. Therefore, we extend the mass balance equations with the diffusion-limited reaction rate constants for describing the retention of H and D atoms under simultaneous dual H^+ and D^+ ion irradiation. A set of the mass balance equations for the local concentrations of activated hydrogen isotopes (n^{H} and n^{D}) and trapped ones ($n_{\mathrm{T}}^{\mathrm{H}}$ and $n_{\mathrm{T}}^{\mathrm{D}}$) are expressed in terms of the following equations:

$$\begin{aligned}\frac{\mathrm{d}n^{\mathrm{H}}}{\mathrm{d}t} = {} & \Sigma_{\mathrm{d}}^{\mathrm{H}} n_{\mathrm{T}}^{\mathrm{H}} + \phi^{\mathrm{H}}\sigma_{\mathrm{d}}^{\mathrm{HH}} n_{\mathrm{T}}^{\mathrm{H}} + \phi^{\mathrm{D}}\sigma_{\mathrm{d}}^{\mathrm{DH}} n_{\mathrm{T}}^{\mathrm{H}} - \Sigma_{\mathrm{T}}^{\mathrm{H}}\left(C_0 - n_{\mathrm{T}}^{\mathrm{H}} - n_{\mathrm{T}}^{\mathrm{D}}\right)n^{\mathrm{H}} - K^{\mathrm{HH}} n^{\mathrm{H}} n_{\mathrm{T}}^{\mathrm{H}} - K^{\mathrm{HD}} n^{\mathrm{H}} n_{\mathrm{T}}^{\mathrm{D}} - 2K_{\mathrm{l}}^{\mathrm{HH}} n^{\mathrm{H}} n^{\mathrm{H}} \\ & - K_{\mathrm{l}}^{\mathrm{HD}} n^{\mathrm{H}} n^{\mathrm{D}} - \alpha R^{\mathrm{H}} n_{\mathrm{T}}^{\mathrm{H}} n^{\mathrm{H}} - \alpha R^{\mathrm{H}} n_{\mathrm{T}}^{\mathrm{D}} n^{\mathrm{H}} + \frac{\phi^{\mathrm{H}}}{\Delta R^{\mathrm{H}}},\end{aligned} \tag{1}$$

$$\begin{aligned}\frac{\mathrm{d}n_{\mathrm{T}}^{\mathrm{H}}}{\mathrm{d}t} = {} & -\Sigma_{\mathrm{d}}^{\mathrm{H}} n_{\mathrm{T}}^{\mathrm{H}} - \phi^{\mathrm{H}}\sigma_{\mathrm{d}}^{\mathrm{HH}} n_{\mathrm{T}}^{\mathrm{H}} - \phi^{\mathrm{D}}\sigma_{\mathrm{d}}^{\mathrm{DH}} n_{\mathrm{T}}^{\mathrm{H}} + \Sigma_{\mathrm{T}}^{\mathrm{H}}\left(C_0 - n_{\mathrm{T}}^{\mathrm{H}} - n_{\mathrm{T}}^{\mathrm{D}}\right)n^{\mathrm{H}} - K^{\mathrm{HH}} n^{\mathrm{H}} n_{\mathrm{T}}^{\mathrm{H}} - K^{\mathrm{DH}} n^{\mathrm{D}} n_{\mathrm{T}}^{\mathrm{H}} - \alpha R^{\mathrm{H}}\beta^{\mathrm{H}} n_{\mathrm{T}}^{\mathrm{H}} n^{\mathrm{H}} \\ & - \alpha R^{\mathrm{D}}\beta^{\mathrm{H}} n_{\mathrm{T}}^{\mathrm{H}} n^{\mathrm{D}},\end{aligned} \tag{2}$$

$$\begin{aligned}\frac{\mathrm{d}n^{\mathrm{D}}}{\mathrm{d}t} = {} & \Sigma_{\mathrm{d}}^{\mathrm{D}} n_{\mathrm{T}}^{\mathrm{D}} + \phi^{\mathrm{H}}\sigma_{\mathrm{d}}^{\mathrm{HD}} n_{\mathrm{T}}^{\mathrm{D}} + \phi^{\mathrm{D}}\sigma_{\mathrm{d}}^{\mathrm{DD}} n_{\mathrm{T}}^{\mathrm{D}} - \Sigma_{\mathrm{T}}^{\mathrm{D}}\left(C_0 - n_{\mathrm{T}}^{\mathrm{H}} - n_{\mathrm{T}}^{\mathrm{D}}\right)n^{\mathrm{D}} - K^{\mathrm{DD}} n^{\mathrm{D}} n_{\mathrm{T}}^{\mathrm{D}} - K^{\mathrm{DH}} n^{\mathrm{D}} n_{\mathrm{T}}^{\mathrm{H}} - 2K_{\mathrm{l}}^{\mathrm{DD}} n^{\mathrm{D}} n^{\mathrm{D}} \\ & - K_{\mathrm{l}}^{\mathrm{HD}} n^{\mathrm{D}} n^{\mathrm{H}} - \alpha R^{\mathrm{D}} n_{\mathrm{T}}^{\mathrm{D}} n^{\mathrm{D}} - \alpha R^{\mathrm{D}} n_{\mathrm{T}}^{\mathrm{H}} n^{\mathrm{D}} + \frac{\phi^{\mathrm{D}}}{\Delta R^{\mathrm{D}}},\end{aligned} \tag{3}$$

$$\begin{aligned}\frac{\mathrm{d}n_{\mathrm{T}}^{\mathrm{D}}}{\mathrm{d}t} = {} & -\Sigma_{\mathrm{d}}^{\mathrm{D}} n_{\mathrm{T}}^{\mathrm{D}} - \phi^{\mathrm{H}}\sigma_{\mathrm{d}}^{\mathrm{HD}} n_{\mathrm{T}}^{\mathrm{D}} - \phi^{\mathrm{D}}\sigma_{\mathrm{d}}^{\mathrm{DD}} n_{\mathrm{T}}^{\mathrm{D}} + \Sigma_{\mathrm{T}}^{\mathrm{D}}\left(C_0 - n_{\mathrm{T}}^{\mathrm{H}} - n_{\mathrm{T}}^{\mathrm{D}}\right)n^{\mathrm{D}} - K^{\mathrm{DD}} n^{\mathrm{D}} n_{\mathrm{T}}^{\mathrm{D}} - K^{\mathrm{HD}} n^{\mathrm{H}} n_{\mathrm{T}}^{\mathrm{D}} - \alpha R^{\mathrm{D}}\beta^{\mathrm{D}} n_{\mathrm{T}}^{\mathrm{D}} n^{\mathrm{D}} \\ & - \alpha R^{\mathrm{H}}\beta^{\mathrm{D}} n_{\mathrm{T}}^{\mathrm{D}} n^{\mathrm{H}},\end{aligned} \tag{4}$$

where C_0 is the trap concentration, ϕ^{H} and ϕ^{D} are the implantation fluxes of H^+ and D^+, $\phi^{\mathrm{H}}/\Delta R^{\mathrm{H}}$ and $\phi^{\mathrm{D}}/\Delta R^{\mathrm{D}}$ are the source terms of H^+ and D^+ ions (ΔR^{H} and ΔR^{D} represent the range straggling for H^+ and D^+ ions), $\sigma_{\mathrm{d}}^{\mathrm{HH}}$ and $\sigma_{\mathrm{d}}^{\mathrm{HD}}$ are the H^+ ion-induced detrapping cross-sections for trapped H and D atoms and $\sigma_{\mathrm{d}}^{\mathrm{DH}}$ and $\sigma_{\mathrm{d}}^{\mathrm{DD}}$ are the D^+ ion-induced detrapping cross-sections for trapped H and D atoms, $\Sigma_{\mathrm{T}}^{\mathrm{H}}$ and $\Sigma_{\mathrm{T}}^{\mathrm{D}}$ are the trapping rate constants for H and D atoms, $\Sigma_{\mathrm{d}}^{\mathrm{H}}$ and $\Sigma_{\mathrm{d}}^{\mathrm{D}}$ are the thermal detrapping rate constants for trapped H and D atoms, K^{HH}, K^{DD}, K^{HD} and K^{DH} represent the rate constants of local molecular recombination between a mobile species and a trapped one in the form of H_2, D_2 and HD, respectively. $K_{\mathrm{l}}^{\mathrm{HH}}$, $K_{\mathrm{l}}^{\mathrm{DD}}$ and $K_{\mathrm{l}}^{\mathrm{HD}}$ represent the rate constants of molecular recombination between mobile hydrogen isotopes in the form of H_2, D_2 and HD, respectively. R^{H} and R^{D} are the rate constants of hydrocarbon molecule formation for mobile H and D atoms to be trapped into a precursor of hydrogen-target complex, α is the fraction of hydrogen atoms in the precursor to total trapped hydrogen atoms and β^{H} and β^{D} represent the number of H and D atoms in the precursor. The break-up of methane by incident ions, observed recently by the Haasz group [22,23], is taken into account indirectly via ion-induced detrapping of trapped hydrogen atoms in the precursor. The atomic re-emission of hydrogen was not taken into account, because the experiments were below 900 K. All the rate constants except α, β^{H} and β^{D} included in Eqs. (1)–(4) were experimentally obtained or were theoretically calculated on the diffusion limited reaction model.

4.2. The D/H ratio

4.2.1. Graphite at low temperature

At room temperature, the contribution of thermally activated processes, such as thermal detrapping, local molecular recombination and formation of hydrogen-target complex molecule, to the hydrogen re-emission is significantly small so as to be neglected. The re-emission of trapped species only takes place through local molecular recombination with species activated due to ion-induced detrapping, which are energetic and athermal. Since the trapping rate constant is extremely large compared with the detrapping rate and the molecular recombination rate, it is assumed that n^{H} and n^{D} reach a quasi-equilibrium just after the start of H^+ and D^+ ion implantation, namely $\mathrm{d}n^{\mathrm{H}}/\mathrm{d}t = 0$ and $\mathrm{d}n^{\mathrm{D}}/\mathrm{d}t = 0$. Using the conditions that $\mathrm{d}(n^{\mathrm{H}} + n_{\mathrm{T}}^{\mathrm{H}})/\mathrm{d}t = 0$ and $\mathrm{d}(n^{\mathrm{D}} + n_{\mathrm{T}}^{\mathrm{D}})/\mathrm{d}t = 0$, the ratio of $n_{\mathrm{T}}^{\mathrm{H}}$ to $n_{\mathrm{T}}^{\mathrm{D}}$ at steady state is expressed by the following equation [16]:

$$\frac{n_{\mathrm{T}}^{\mathrm{H}}}{n_{\mathrm{T}}^{\mathrm{D}}} = \frac{\left(K^{\mathrm{DD}}/\Sigma_{\mathrm{T}}^{\mathrm{D}}\right)}{\left(K^{\mathrm{HH}}/\Sigma_{\mathrm{T}}^{\mathrm{H}}\right)} \frac{\left\{1 + \left(\Delta R^{\mathrm{D}}/\Delta R^{\mathrm{H}}\right)\left(\phi^{\mathrm{H}}/\phi^{\mathrm{D}}\right) + 2\left(\sigma_{\mathrm{d}}{}^{\mathrm{DD}} + \sigma_{\mathrm{d}}{}^{\mathrm{HD}}\left(\phi^{\mathrm{H}}/\phi^{\mathrm{D}}\right)\right) n_{\mathrm{T}}^{\mathrm{D}} \Delta R^{\mathrm{D}}\right\}}{\left\{1 + \left(\Delta R^{\mathrm{H}}/\Delta R^{\mathrm{D}}\right)\left(\phi^{\mathrm{D}}/\phi^{\mathrm{H}}\right) + 2\left(\sigma_{\mathrm{d}}{}^{\mathrm{HH}} + \sigma_{\mathrm{d}}{}^{\mathrm{DH}}\left(\phi^{\mathrm{D}}/\phi^{\mathrm{H}}\right)\right) n_{\mathrm{T}}^{\mathrm{H}} \Delta R^{\mathrm{H}}\right\}}. \tag{5}$$

The value of $n_{\mathrm{T}}^{\mathrm{H}}/n_{\mathrm{T}}^{\mathrm{D}}$ was obtained using the experimental values of $K^{\mathrm{HH}}/\Sigma_{\mathrm{T}}^{\mathrm{H}} = 0.2$, $K^{\mathrm{DD}}/\Sigma_{\mathrm{T}}^{\mathrm{D}} = 0.1$, $\sigma_{\mathrm{d}}{}^{\mathrm{HD}} = 2.5 \times 10^{-18}$ cm^2, $\sigma_{\mathrm{d}}{}^{\mathrm{DH}} = 3.3 \times 10^{-18}$ cm^2 and $\sigma_{\mathrm{d}}{}^{\mathrm{HH}} = \sigma_{\mathrm{d}}{}^{\mathrm{DD}} = 2.9 \times 10^{-18}$ cm^2 [16,24,25] and the experimental conditions $\Delta R^{\mathrm{H}}/\Delta R^{\mathrm{D}} = 0.8$ and $\phi^{\mathrm{H}}/\phi^{\mathrm{D}} \cong 1$ (including the reflection coefficients). The value of $n_{\mathrm{T}}^{\mathrm{D}}/n_{\mathrm{T}}^{\mathrm{H}}$ calculated self-consistently from Eq. (5) was 1.5, which is a little bit smaller than the experimental one. The difference is ascribed to dropping of the diffusion term from the mass balance equations for simplicity.

4.2.2. Graphite at elevated temperatures

At elevated temperatures, the concentrations of hydrogen isotopes retained decrease due to increase of the rate constants of thermally activated processes for re-emission such as thermal detrapping, local molecular recombination between mobile species and hydrocarbon molecule formation, which are major processes at temperatures above 700 K in the present study, because the implantation flux is only 4.3×10^{13} ions/cm^2 s. According to the diffusion-limited reaction model, it is assumed that R^{H} and R^{D} are expressed by the relations $R^{\mathrm{H}} = 4\pi r_{\mathrm{HC}} D^{\mathrm{H}}$ and $R^{\mathrm{D}} = 4\pi r_{\mathrm{HC}} D^{\mathrm{D}}$, respectively, where r_{HC} is the effective radius of the precursor for hydrocarbon molecule formation [19]. On the other hand, $\Sigma_{\mathrm{T}}^{\mathrm{H}} = 4\pi r_{\mathrm{T}} D^{\mathrm{H}}$ and $\Sigma_{\mathrm{T}}^{\mathrm{D}} = 4\pi r_{\mathrm{T}} D^{\mathrm{D}}$, where r_{T} is the effective radius of the trap. When $r_{\mathrm{HC}} = r_{\mathrm{T}}$, $R^{\mathrm{H}} = \Sigma_{\mathrm{T}}^{\mathrm{H}}$ and $R^{\mathrm{D}} = \Sigma_{\mathrm{T}}^{\mathrm{D}}$. Under such a condition, the ratio of D to H retained at steady state is expressed by the following equation:

$$\frac{\Delta R^{\mathrm{H}}}{\Delta R^{\mathrm{D}}} = \frac{\left[2\left(K_{\mathrm{l}}^{\mathrm{HH}}/C_0\right)\left(\Sigma_{\mathrm{d}}^{\mathrm{H}}/\Sigma_{\mathrm{T}}^{\mathrm{H}}\right)^2 + \alpha\left(1 + \beta^{\mathrm{H}}\right)\Sigma_{\mathrm{d}}^{\mathrm{H}}\right] x^2 + \left[\left(K_{\mathrm{l}}^{\mathrm{HD}}/C_0\right)\left(\Sigma_{\mathrm{d}}^{\mathrm{H}}/\Sigma_{\mathrm{T}}^{\mathrm{H}}\right)\left(\Sigma_{\mathrm{d}}^{\mathrm{D}}/\Sigma_{\mathrm{T}}^{\mathrm{D}}\right) + \alpha\Sigma_{\mathrm{d}}^{\mathrm{H}} + \alpha\beta^{\mathrm{H}}\Sigma_{\mathrm{d}}^{\mathrm{D}}\right] x}{\left[2\left(K_{\mathrm{l}}^{\mathrm{DD}}/C_0\right)\left(\Sigma_{\mathrm{d}}^{\mathrm{D}}/\Sigma_{\mathrm{T}}^{\mathrm{D}}\right)^2 + \alpha\left(1 + \beta^{\mathrm{D}}\right)\Sigma_{\mathrm{d}}^{\mathrm{D}}\right] + \left[\left(K_{\mathrm{l}}^{\mathrm{HD}}/C_0\right)\left(\Sigma_{\mathrm{d}}^{\mathrm{H}}/\Sigma_{\mathrm{T}}^{\mathrm{H}}\right)\left(\Sigma_{\mathrm{d}}^{\mathrm{D}}/\Sigma_{\mathrm{T}}^{\mathrm{D}}\right) + \alpha\Sigma_{\mathrm{d}}^{\mathrm{D}} + \alpha\beta^{\mathrm{D}}\Sigma_{\mathrm{d}}^{\mathrm{H}}\right] x}, \tag{6}$$

where $x = n_{\mathrm{T}}^{\mathrm{H}}/n_{\mathrm{T}}^{\mathrm{D}}$. The values of the effective molecular recombination rate constants $2(K_{\mathrm{l}}^{\mathrm{ii}}/C_0)(\Sigma_{\mathrm{d}}^{\mathrm{i}}/\Sigma_{\mathrm{T}}^{\mathrm{i}})^2$ are by three orders of magnitude smaller than the values of $\Sigma_{\mathrm{d}}^{\mathrm{i}}$, which were experimentally found in the isothermal re-emission experiments on H and D implanted into graphite at room temperature up to saturation [20]. Since it was also experimentally shown that $\Sigma_{\mathrm{T}}^{\mathrm{H}}/\Sigma_{\mathrm{T}}^{\mathrm{D}} = \sqrt{2}$ and $C_0 \gg n_{\mathrm{T}}^{\mathrm{H}} + n_{\mathrm{T}}^{\mathrm{D}}$ [19], it follows that

$$\left(1 + \beta^{\mathrm{H}}\right)\sqrt{2}\, x^2 + \left[\left(\sqrt{2} + \beta^{\mathrm{H}}\right) - f\left(1 + \beta^{\mathrm{D}}\sqrt{2}\right)\right] x - f\left(1 + \beta^{\mathrm{D}}\right) = 0, \tag{7}$$

where $f = \Delta R^{\mathrm{D}}/\Delta R^{\mathrm{H}}$ which is 1.25 in the present study. This equation indicates that the value of x is determined from the values of $\beta^{\mathrm{H}}/\beta^{\mathrm{D}}$ and vice versa. We have no data on β^{H} and β^{D} yet. There is only one measurement of mixed-isotope methane formation during simultaneous H^+ and D^+ bombardment by Chiu et al. [26]. We cannot extract the values of β^{H} and β^{D} from their data. The values of β^{H} and β^{D} are calculated to be 2.1 and 1.09, respectively for $x = 1.5$, which is equal to the room temperature value. This fact might indicate that the H/D ratio in the precursor is no less than 2.1/0.9.

4.2.3. Beryllium at room temperature

In the previous section, the saturation concentrations of H and D retained in beryllium by independent ion implantation at room temperature were found to be $\sim 5 \times 10^{22}$/cm^3. Most of the hydrogen isotopes retained were found to be re-emitted due to thermal annealing up to 600 K [9,27]. These facts indicate that the trapping rate is extremely high compared with the ion-induced detrapping rate and the molecular recombination rate. Beryllium targets implanted with D^+ ions up to saturation were heavily damaged and the damaged region included vacancy clusters such as cavities, voids and bubbles. Therefore the recombination may take place at the inner surface of the damaged region, which is very consistent with the fact that the thermal re-emission rate from beryllium is not dependent on the depth. These facts indicate that the mass balance equations for beryllium are very similar to those for graphite at elevated temperatures except the detrapping is ion-induced and no emission of hydrogen-metal complexes takes place.

According to above considerations, the ratio of H and D retained in beryllium at room temperature by simultaneous H^+

and D^+ implantation is expressed, as a solution of Eqs. (1)–(4) at steady state under the condition that R^H and $R^D = 0$, by the following equation:

$$\frac{\Delta R^{H}}{\Delta R^{D}} = \frac{2K_{l}^{HH}\left(\sigma_{d}{}^{H}/\Sigma_{T}^{H}\right)^{2}x^{2} + K_{l}^{HD}\left(\sigma_{d}{}^{H}/\Sigma_{T}^{H}\right)\left(\sigma_{d}{}^{D}/\Sigma_{T}^{D}\right)x}{2K_{l}^{DD}\left(\sigma_{d}{}^{D}/\Sigma_{T}^{D}\right)^{2} + K_{l}^{HD}\left(\sigma_{d}{}^{H}/\Sigma_{T}^{H}\right)\left(\sigma_{d}{}^{D}/\Sigma_{T}^{D}\right)x}, \tag{8}$$

where $\sigma_d{}^H = \sigma_d{}^{HH} + \sigma_d{}^{DH}$, $\sigma_d{}^D = \sigma_d{}^{DD} + \sigma_d{}^{HD}$. According to the diffusion-limited reaction model, it is assumed that $K_l^{HH} = 4\pi r_R^{HH} D^H \xi^{HH}$, $K_l^{DD} = 4\pi r_R^{DD} D^D \xi^{DD}$ and $K_l^{HD} = 4\pi r_R^{HD} D^{HD} \xi^{HD}$, where r_R^{ij} are the effective radii for recombination between mobile species i and j, enhanced by a factor of $\sqrt{D^i + D^j}$, ξ^{ij} are the formation probability for a molecule ij and $D^{HD} = (D^H + D^D)/2$, thus $(K_l^{HD})^2/K_l^{HH}K_l^{DD} = (1 + D^D/D^H)(1 + D^H/D^D)(\sqrt{D^D/D^H} + \sqrt{D^H/D^D})/8$. With use of the above relations, the ratio n_T^D/n_T^H is expressed by following equation:

$$\frac{n_T^H}{n_T^D} = \sqrt{\frac{K_l^{DD}\left(\sigma_d{}^D/\Sigma_T^D\right)^2}{K_l^{HH}\left(\sigma_d{}^H/\Sigma_T^H\right)^2}}\left(\sqrt{1 + \frac{(1-f)^2}{16}\frac{\left(K_l^{HD}\right)^2}{K_l^{HH}K_l^{DD}}} - \frac{(1-f)}{4}\frac{K_l^{HD}}{\sqrt{K_l^{HH}K_l^{DD}}}\right), \tag{9}$$

where $f = \Delta R^D/\Delta R^H$ which is 1.25 in the present experiment.

The isotope ratio of $K_l^{ii}(\sigma_d{}^i/\Sigma_T^i)^2$ for graphite [18] may be used for beryllium, because it is theoretically expected that the isotope ratio for graphite is the same as that for beryllium, although the absolute rate constants for beryllium and graphite are quite different. In such a case the ratio n_T^D/n_T^H is estimated to be 1.3, which is very consistent with the experimental one. Finally, it is noted that the rate constants of elementary processes for hydrogen retention and re-emission are needed.

In conclusion, the agreement between the experimental and calculated isotope ratios in the steady state retention by simultaneous dual H^+ and D^+ irradiation is concluded to indicate that the diffusion-limited reaction model is reasonable for description of the rate constants. The large isotope ratio for graphite is ascribed to the local molecular recombination between a mobile species and a trapped one at low temperature and emission of hydrocarbon molecule at elevated temperature, which are major elementary processes for re-emission.

References

[1] The JET Team, J. Nucl. Mater. 196–198 (1992) 3.

[2] The TFTR Group, Proc. 11th Int. Conf. Plasma Surface Interactions in Controlled Fusion Devices, May 23–27, Mito, Japan (1994), to be published.

[3] W. Möler, J. Nucl. Mater. 162–164 (1989) 138.

[4] R.A. Causey, J. Nucl. Mater. 162–164 (1989) 151.

[5] K.L. Wilson et al., Nucl. Fusion (Suppl.) 1 (1991) 31.

[6] W. Möler and B.M.U. Scherzer, Appl. Phys. Lett. 50 (1987) 1870.

[7] Ch. Wild and P. Koidl, Appl. Phys. Lett. 51 (1987) 1506.

[8] K. Morita and Y. Hasebe, J. Nucl. Mater. 176–177 (1990) 213.

[9] W.R. Wampler, J. Nucl. Mater. 122–123 (1984) 213.

[10] W.R. Wampler, J. Nucl. Mater. 196–198 (1992) 983.

[11] J. Roth and J. Bohdansky, Appl. Phys. Lett. 51 (1987) 13.

[12] W. Möler and B.M.U. Sckerzer, J. Appl. Phys. 64 (1988) 4860.

[13] K. Morita and Y. Hasebe, Mem. Fac. Eng. Nagoya Univ. 45 (1993) 57.

[14] K. Morita, K. Ohtsuka and Y. Hasebe, J. Nucl. Mater. 162–164 (1989) 990.

[15] A.A. Haasz, P. Franzen, J.A. Davies, S. Chiu and C.S. Pitcher, J. Appl. Phys. 77 (1995) 66.

[16] B. Tsuchiya and K. Morita, J. Nucl. Mater. 227 (1996) 195.

[17] H.H. Andersen and J.F. Ziegler, Hydrogen Stopping Powers and Ranges in All Elements (Plenum, New York, 1977).

[18] S. Nagata et al., Nucl. Instr. Methods B 6 (1985) 533.

[19] Y. Muto and K. Morita, J. Nucl. Mater. 223 (1995) 262.

[20] K. Morita and Y. Muto, J. Nucl. Mater. 196–198 (1992) 963.

[21] E. Abramov et al., J. Nucl. Mater. 175 (1990) 90.

[22] S. Chiu, A.A. Haasz and P. Franzen, J. Nucl. Mater. 218 (1995) 319.

[23] A.A. Haasz and P. Franzen, J. Nucl. Mater. 220–222 (1995) 815.

[24] B. Tsuchiya and K. Morita, J. Nucl. Sci. Technol. 31 (1994) 1301.

[25] B. Tsuchiya and K. Morita, J. Nucl. Mater. 226 (1995) 298.

[26] S. Chiu and A.A. Haasz, J. Nucl. Mater. 208 (1994) 282.

[27] B. Tsuchiya and K. Morita, J. Nucl. Mater. (1996), in press.